

Engineering Notes

ENGINEERING NOTES are short manuscripts describing new developments or important results of a preliminary nature. These Notes should not exceed 2500 words (where a figure or table counts as 200 words). Following informal review by the Editors, they may be published within a few months of the date of receipt. Style requirements are the same as for regular contributions (see inside back cover).

Flow Control by Spanwise Blowing on a NACA 0012

C. Wong* and K. Kontis†

University of Manchester, Manchester, M60 1QD England,
United Kingdom

DOI: 10.2514/1.25227

Introduction

THE initial study of lateral steady blowing was conducted by Dixon [1] in 1969. The mechanism of the concept is analogous to the flow over slender delta wing platforms, which produces a leading-edge vortex and nonlinear lift curves. Spanwise steady blowing might be thought of as providing the sweep effects similar to that of the delta wings, for which the effective sweep is a function of the jet momentum. The spanwise blowing jet can be described in terms of the chordwise position along the airfoil section, the nozzle height, and the nozzle size. Dixon et al [2] and Clarke [3] suggested that the best vertical nozzle position may well be a function of nozzle diameter, and that the jet from a nozzle placed too near the wing surface may well have a deleterious effect on the airflow over the wing. The large momentum needed to generate a lift increase is a major issue in the effectiveness of the blowing, and as a consequence, Meyer and Seginer [4] performed some initial tests for generating the same lift increase using a lower momentum by way of pulsating blowing. The objectives of the present Note are to expand the existing experimental database and to extend the understanding of the effects of spanwise steady and unsteady blowing on the aerodynamic performance. The present topic is the subject of ongoing research.

Experimental Setup

Measurements were conducted in a subsonic blown-down wind-tunnel facility with freestream turbulent intensity of 0.28% at a freestream velocity of 12 m/s. A NACA 0012 airfoil with a span of 451 mm and chord length of 151 mm was employed. The Reynolds number based on the chord length is 1.25×10^5 . The airfoil was manufactured and polished to a smooth finish. No boundary-layer trips were employed, because the experiments were intended to demonstrate the effect and to examine the efficiency of the application of spanwise steady and unsteady blowing on the aerodynamic performance. The tests were performed in a transition-free condition. Spanwise blowing was realized by injecting a pair of

sonic jets in parallel to the span of the airfoil. The blowing jet nozzle was of circular cross section, with an internal diameter of 4 mm. It was situated 1 mm above the surface of the airfoil. Three nozzle positions were tested: $x/c = 0, 0.25$, and 1, where c is the chord length and x is the Cartesian coordinate along the chord line of the airfoil. A compressor supplied the air for the jet via a series of pressure manifolds. The unsteady blowing system employed an oscillator valve with logic functions. The unsteady air jet was fluctuated as a sinusoid wave, and the tests were conducted at frequencies equal to 8, 12, and 16 Hz. The blowing pressure was kept constant to 2 bar for both steady and unsteady cases. Aerodynamic forces were measured by a three-component external strain gauge balance connected to a 12-bit data acquisition system, with a sampling rate of 10 kHz. Aerodynamic forces were normalized by the freestream dynamic pressure q and airfoil area S . They were not corrected for jet direct thrust. For unsteady blowing measurements, mean lift and mean drag coefficients were calculated. The jet-momentum coefficient C_{μ} is equal to $\dot{m}_j V_j / qS$, where \dot{m}_j is the mass flow rate of the blowing jet and V_j is the jet velocity. Both steady and unsteady blowing systems were extensively calibrated, and the mean mass flow rates and mean jet velocities were recorded. For surface flow visualization, the oil flow technique was employed. Boundary-layer properties were measured with a two-component slanted sensor hot-wire anemometry (TSI IFA-100 intelligent flow analyzer), and data were taken for 1 s, at a sampling rate of 10 kHz.

Results

Force Balance

Figure 1a shows that the maximum lift coefficient $C_{L\max}$ of the steady-blowing cases is higher than that of the no-blowing case. For the steady blowing applied at $x/c = 0$, the C_L curve overlaps the curve corresponding to the no-blowing case, up to 9-deg incidence, and the stall angle is postponed to 11 deg. This is because the mass flux from the blowing jet flows over both the upper and lower surfaces of the airfoil equally; thus, the mean velocity on the airfoil surfaces is increased and, therefore, $C_{L\max}$ and stall angle are also increased. The elimination of the stagnation point occurs at the leading edge of the airfoil near the blowing nozzle and it appears near the downstream, due to the increasing mass flow entrainment and jet mixing on the airfoil surface as the flow moves outboard. On the other hand, the characteristics of nonlinearity of the curves occurred for blowing at $x/c = 0.25$ and 1, except for the finite value of lift produced at zero angle of attack. The increase of C_L due to blowing at $x/c = 0.25$ is observed in Fig. 1a, and it can be explained by the deflection of streamlines over the upper surface of the airfoil, the camber of which increases aft of the quarter chord of the airfoil. This camber is apparently the effect of entraining freestream air into the jet. For the blowing at $x/c = 1$, almost the same rate of increase of C_L with the no-blowing case is observed. The trailing-edge spanwise blowing increases the negative pressure on the upper surface of the airfoil, due to the accelerated flow. The blowing jet works as an obstacle lying laterally against the main flow. Thus, the pressure on the lower surface increases and overall lift is increased, as a result. The drag from the steady-blowing cases is increased compared with the no-blowing case, except at zero angle of attack for blowing applied at $x/c = 0.25$. At zero angle of attack, the drag for spanwise blowing at $x/c = 0.25$ is actually lower than the no-blowing case. This case study has been unable to confirm the occurrence of

Received 17 May 2006; revision received 25 August 2006; accepted for publication 29 August 2006. Copyright © 2006 by C. Wong and K. Kontis. Published by the American Institute of Aeronautics and Astronautics, Inc., with permission. Copies of this paper may be made for personal or internal use, on condition that the copier pay the \$10.00 per-copy fee to the Copyright Clearance Center, Inc., 222 Rosewood Drive, Danvers, MA 01923; include the code \$10.00 in correspondence with the CCC.

*Research Student, School of Mechanical, Aerospace and Civil Engineering. Student Member AIAA.

†Associate Professor (Senior Lecturer), School of Mechanical, Aerospace and Civil Engineering. Member AIAA.

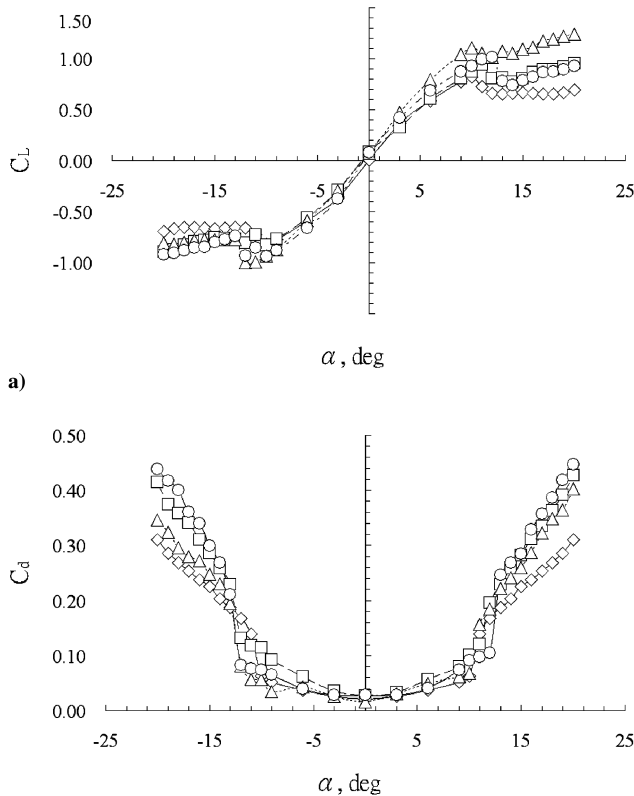


Fig. 1 Comparison of aerodynamic forces for the airfoil with steady blowing ($C_\mu = 0.197$) and no blowing ($C_\mu = 0$): a) C_L vs α and b) C_d vs α ; (\diamond , no blowing; \square , $x/c = 0$; \triangle , $x/c = 0.25$; and \circ , $x/c = 1$).

reduction of drag; however, other researchers have observed similar results in their studies (Fig. 1b).

Figure 2 shows the variation of blowing efficiency $\Delta C_L/C_\mu$, with incidence for different jet locations along the chord. When $\Delta C_L/C_\mu > 1$, blowing is efficient, and when $\Delta C_L/C_\mu < 1$, blowing is inefficient. The blowing efficiency is higher than one when the blowing is applied at $x/c = 0.25$ for all positive incidences. The blowing efficiency is larger than one when blowing is applied at $x/c = 0$ and is equal to one for angles of attack above 11 deg. Consequently, the spanwise blowing is considered as an efficient technique for improving the performance of the airfoil at high angles of attack, and it works effectively in the reversed flow region. The effect of spanwise unsteady blowing is examined in Fig. 3. It can be seen that the C_L is reduced when unsteady blowing is applied at $x/c = 0.25$; this is because the mean C_μ for the unsteady blowing is smaller than that for the steady blowing. Although the unsteady momentum coefficients vary according to the mass flow rate, the

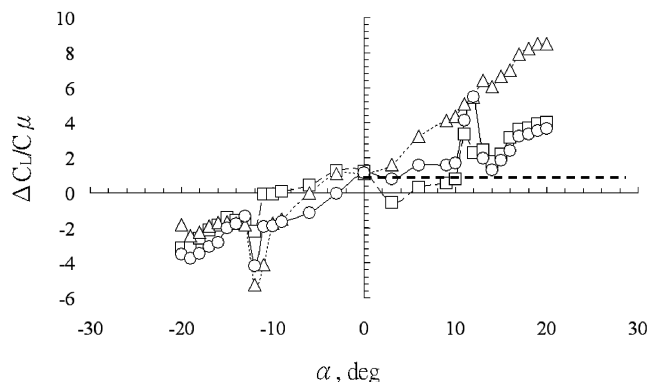


Fig. 2 Blowing efficiency for the airfoil with steady blowing; (\square , $x/c = 0$; \triangle , $x/c = 0.25$; and \circ , $x/c = 1$).

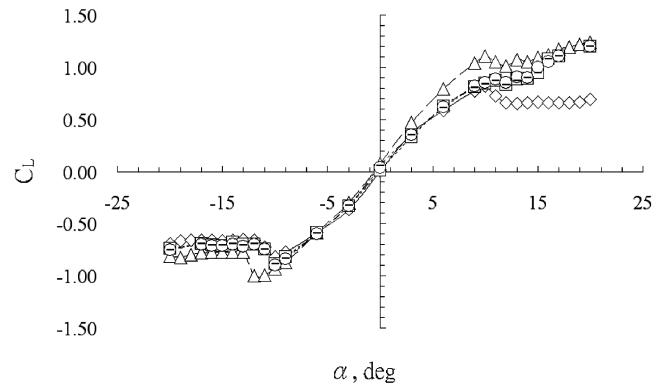


Fig. 3 Comparison of mean lift coefficients for the airfoil with no blowing ($C_\mu = 0$), steady blowing ($C_\mu = 0.197$), and unsteady blowing; (\diamond , no blowing; \triangle , steady blowing; \square , unsteady blowing (8 Hz, $C_\mu = 0.084$); \circ , unsteady blowing (12 Hz, $C_\mu = 0.134$); and solid line, unsteady blowing (16 Hz, $C_\mu = 0.146$)).

unsteady blowing does not significantly influence the unsteady behavior of C_L . On the other hand, the low-frequency range tested may constrain the effect of the unsteady behavior of C_L . C_L at 16 Hz for zero angle of attack is higher than the other frequencies; this is because the mean mass flux from the blowing-jet entrainment with the freestream jet is the highest at 16 Hz. The stall angle is postponed from 10 to 11 deg when the unsteady blowing is applied. It is thought that the quasi-periodic oscillation in the flow separation bubble on the airfoil section is disturbed by the unsteady blowing jet; thus, the unsteady blowing jet suppresses the natural flow oscillations and delays the stall angle of the airfoil.

Oil Flow Visualization

Figure 4a shows that the flow separates near the leading edge and a reversed flow is established. The result of such reversed flow phenomena is to cause the flow to separate from the surface and

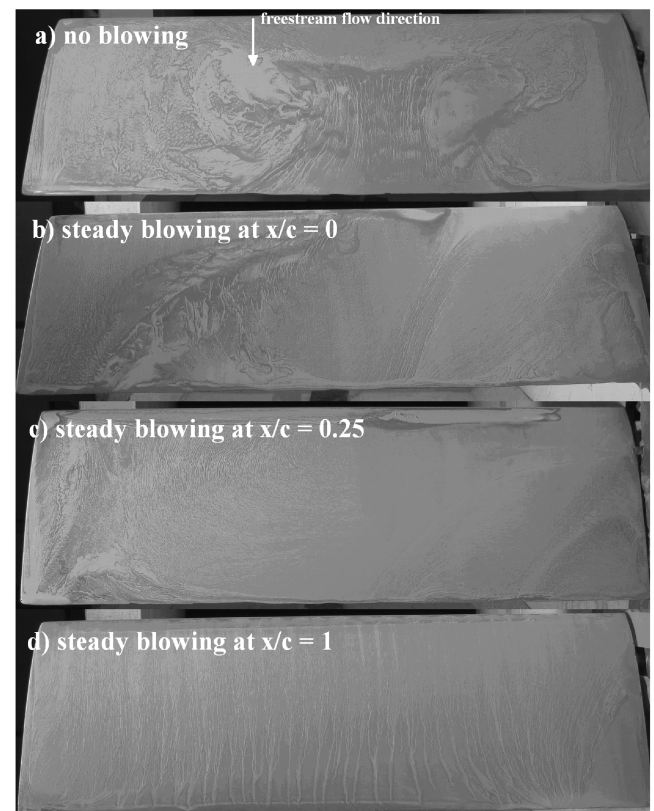


Fig. 4 Surface oil flow visualization for different cases at $\alpha = 12$ deg.

create a large wake of recirculating flow downstream of the surface. It also provides evidence that the airfoil is stalled before or at a 12-deg angle of attack. Figure 4b shows that the blowing jet affects the flow region for less than half of the airfoil. A large separation bubble occurred at the leading edge, which may result in a loss of lift. Moreover, the separated flow on the left-hand side collides with the blowing jet; thus, a violent mixing region is generated. In contrast, it can be seen that a laminar flow pattern is generated in Fig. 4c. The steady blowing applied at $x/c = 0.25$ forms a large separation bubble at the leading edge of the airfoil, due to the strong spanwise blowing jet blowing across the airfoil; thus, the flow is forced to reattach to the surface of the airfoil. Figure 4d shows that the trailing-edge blowing prevents the occurrence of the flow separation on the surface of the airfoil. This phenomenon occurs because of the strong trailing-edge blowing, which blows to the other end of the airfoil and mixes with freestream flow. Thus, the freestream flow becomes highly entrained, reducing the rate of pressure increment in the freestream flow direction. The attached flow on the surface of the airfoil delays the stalling of the airfoil. Short separation bubbles are formed at the leading edge, because the Reynolds number of the boundary layer at separation is sufficiently greater at the leading edge of the airfoil.

Boundary-Layer Surveys

For the no-blowing case at $\alpha = 9$ deg, the boundary layer remains laminar. When blowing is applied at $x/c = 0$, the boundary-layer thickness δ increases considerably as the flow moves downstream. This is due to the high blowing-jet-momentum entrainment with the freestream flow at the leading edge, which causes a favorable pressure gradient. The high-momentum jet causes the external flow to deflect upwards as it travels along the airfoil; thus, the effective body thickness is increased. The result further suggests that the blowing jet induces instability into the laminar boundary layer, so that it becomes turbulent as soon as it separates and forthwith reattaches itself. Hence, the blowing at $x/c = 0$ delays the flow separation over the rear of the airfoil section. When the blowing is applied at $x/c = 1$, the boundary-layer thickness is maintained at low values compared with the no-blowing case. When the blowing is applied at $x/c = 0.25$, the boundary thickness is similar to the one obtained from the case of blowing at $x/c = 0$; however, the velocity at the edge of the boundary layer δ_{vel} is higher, because the blowing jet is nearer to the probe; thus, higher velocities are registered at this blowing location. The displacement thickness δ^* is also increased moderately.

For the steady blowing applied at $x/c = 0$ and 12-deg incidence, the shape factor for all locations is within a range from 1.22 to 1.75. The displacement thickness remains relatively small, due to the attachment of high-momentum blowing jet, and thus the lift increment is the smallest. At $x/c = 0.25$ and 12-deg incidence, the blowing jet collides with the reversed flow near the trailing edge. The momentum of the reversed flow is cancelled by the streamwise blowing jet, and the momentum thickness is increased, as a result. For the steady blowing applied at $x/c = 1$ and 12-deg incidence, the circulation of the airfoil is altered. The boundary-layer thickness near the leading edge is smaller than the no-blowing case. The stagnation point is pushed onto the upper surface of the airfoil when the trailing-edge blowing is applied. It was found that the shape factor is high for all locations tested, which proves that the high turbulence of the blowing jet creates a favorable condition, causing the flow to remain attached to the surface of the airfoil.

Conclusions

The lift coefficient increases with the application of spanwise steady blowing, and the most effective blowing location was found at $x/c = 0.25$, because the $\Delta C_L/C_{\mu}$ was always above one for all positive angles of attack. Moreover, when the unsteady blowing was applied, the stall angle was postponed from 10 to 11 deg. It is suggested that the unsteady blowing suppresses the flow oscillations near stall. The high-momentum jet mixes with the freestream flow and the jet is deflected. Lateral steady and unsteady blowing is a direct and effective flow control technique for improving the aerodynamic characteristics and performance of airfoils and wings.

References

- [1] Dixon, C. J., "Lift Augmentation by Lateral Blowing over a Lifting Surface," AIAA Paper 69-193, 1969.
- [2] Dixon, C. J., Theisen, J. G., and Scruggs, R. M., "Theoretical and Experimental Investigations of Vortex Lift Control by Spanwise Blowing," Vol. 1, Royal Aeronautical Establishment, Rept. AD-771-290, Bedford, England, U.K., Sept. 1973.
- [3] Clarke, K. P., "Lift Augmentation on a Moderately Swept Wing by Spanwise Blowing," *The Aeronautical Journal*, Vol. 80, No. 790, Oct. 1976, pp. 447-451.
- [4] Meyer, J., and Seginer, A., "Effect of Periodic Spanwise Blowing on Delta-Wing Configuration Characteristics," *AIAA Journal*, Vol. 32, No. 4, Apr. 1994, pp. 708-715.